Acta Geotechnica (2021) 16:2165–2173
https://doi.org/10.1007/s11440-021-01163-3

RESEARCH PAPER

Modification of poroelastic properties in granite by heating–cooling treatment

Fan Zhang[1] · Yuhao Zhang[1,3] · Dawei Hu[2] · Jianfu Shao[3]

Received: 27 May 2020 / Accepted: 7 February 2021 / Published online: 24 February 2021

Abstract
Poroelastic properties play an essential role in interaction between deformation and fluid pressure change in porous rocks. These properties can be affected by microstructural evolution such as porosity change and micro-cracks growth. In this study, the modification of poroelastic properties of a hard rock (granite) is investigated in terms of thermally induced micro-cracks. Granite samples are first subjected to a heating–cooling treatment with different values of temperature. The variations of bulk modulus, stiffness of solid grains and Biot's coefficient of thermally treated samples are determined and analyzed. It is found that both connected and occluded micro-cracks are generated in granite samples. The bulk modulus of porous material is affected by the connected micro-cracks, while the stiffness of solid grains is influenced by the occluded micro-cracks. The Biot's coefficient is affected by the connectivity of micro-cracks. All poroelastic properties evolve with effective mean stress and a non-linear poroelastic law should be defined.

Keywords Biot's coefficient · Granite · Heating–cooling treatment · Micro-cracking · Poroelasticity

1 Introduction

Cracking is an essential mechanism in brittle and hard rocks such as granite. Cracking can be induced by mechanical loading, temperature change and fluid pressure variation. In the present study, the emphasis is put on cracking induced by heating–cooling process and its impact on poroelastic properties. We consider here the case of enhanced geothermal system (EGS) in hot dry rocks (HDR) as an example. Such rocks are located from 2 to 10 km in depth, and the initial temperature can reach 650 °C [16, 26]. The common production technique consists in injecting cold water into HDR layers from an injection well and retrieving heated hot water and steam from a production well [14, 22]. The HDR layers are then subjected to a progressive cooling process, which can be at the origin of cracking of rocks.

According to the previous studies [13, 21, 22, 28, 34–36], the physical and hydromechanical properties of rocks can be significantly affected by heating–cooling induced cracking process. For instance, the elastic modulus and failure strength of rocks are decreased, while the permeability and porosity are enhanced. The nucleation and growth of micro-cracks induced by heating–cooling can be related to the non-uniform thermal expansion of different minerals [2, 9, 11, 18, 19, 27], and to the high temperature gradient generated by rapid change of temperature [3, 12, 30, 32].

On the other hand, for saturated and partially saturated porous rocks, the overall deformation behavior is directly driven by the interaction between skeleton deformation and pore pressure change. This interaction is taken into account in soil-like materials by the empirical effective stress concept of Terzaghi [25]. For the general case of cohesive porous materials such as most rocks, the Biot's poroelastic theory provides the fundamental background for studying fluid-rock coupling in saturated conditions [4, 5, 23]. A

✉ Jianfu Shao
jian-fu.shao@polytech-lille.fr

[1] School of Civil Engineering, Architecture and Environment, Hubei University of Technology, Wuhan, China

[2] State Key Laboratory of Geomechanics and Geotechnical Engineering, Institute of Rock and Soil Mechanics, Chinese Academy of Sciences, Wuhan, China

[3] Laboratory of Multiscale Multiphysics Mechanics, LaMcube, UMR9013, EC Lille, CNRS, University of Lille, 59000 Lille, France

number of subsequent extensions of Biot's theory have been proposed in order to consider material anisotropy, induced damage and plastic deformation [6, 8, 15, 20, 33]. In the case of hard rocks like granite, plastic deformation can generally be neglected. The interaction between rock deformation and pore pressure change can be conveniently described by the poroelastic theory. In this theory, the Biot's coefficient for isotropic materials or Biot's tensor for anisotropic ones is the fundamental coupling parameter. It is an intrinsic property of a porous material and dependent on the elastic properties of porous skeleton and solid grains (or phase). Due to the degradation of solid grains, for instance the growth of micro-cracks induced by heating–cooling, chemical reaction or mechanical loading, the value of Biot's coefficient can be significantly modified. This type of results has been reported in a number of previous studies on different kinds of rocks [1, 17, 31]. However, very few studies have been performed on the characterization of Biot's coefficient of hard rocks subjected to high-temperature heating and water cooling. This is the main objective of the present study. The adopted methodology is based on a macroscopic laboratory testing approach. A typical hard rock, granite, is selected. Granite samples are first subjected to heating and water cooling treatment up to different values of temperature. However, the kinetics of cooling used in this study is quite different with that encountered in EGS. Therefore, the objective here is not to reproduce the real thermal conditions of EGS, and to create micro-cracks in granite samples by using the heating–cooling treatment. The values of bulk modulus and stiffness of solid grains of thermally treated samples are measured by hydrostatic compressive tests. By assuming that the studied granite is an isotropic material, the corresponding values of Biot's coefficient are calculated. Based on experimental data, the variations of elastic properties and Biot's coefficient are first analyzed as functions of heating–cooling treatment temperature and hydrostatic compression stress. These variations are further interpreted in terms of creation and closure of micro-cracks inside the solid grains.

2 Theoretical background and experimental procedure

2.1 Theoretical background

We consider here a linear isotropic porous material under saturated and isothermal conditions. The poroelastic behavior of material under the assumption of small strains is described by the classical Biot's theory which is expressed as follows [4, 5]:

$$\begin{cases} (\sigma_{ij} - \sigma_{ij}^0) = \lambda_b(\mathrm{tr}\boldsymbol{\varepsilon})\delta_{ij} + 2\mu_b\varepsilon_{ij} - b(p_f - p_{f0})\delta_{ij} \\ (p_f - p_{f0}) = M\left(-b\,\mathrm{tr}\boldsymbol{\varepsilon} + \dfrac{m}{\rho_0^f}\right) \end{cases} \quad (1)$$

In these relations, σ_{ij} are components of Cauchy stress tensor, ε_{ij} components of linear strain tensor, and p_f fluid pressure (σ_{ij}^0 and p_{f0} are the values of stress and pore pressure at the reference state). λ_b and μ_b are two Lame's coefficient in drained condition. b and M are respectively the Biot's coefficient and Biot's modulus. m is the fluid mass change per unit volume and ρ_0^f the fluid volumetric mass at the reference state. It is worth noticing that for anisotropic rocks, the scalar Biot's coefficient should be replaced by a second-order Biot's tensor [8, 24, 33]. Applying now the Biot's poroelasticity to hydrostatic state, one gets:

$$\begin{cases} (\sigma_m - \sigma_m^0) = k^b\varepsilon_v - b(p_f - p_{f0}); \quad k^b = \lambda_b + \dfrac{2}{3}\mu_b \\ (p - p_0) = M(-b\varepsilon_v + \dfrac{m}{\rho_0^f}) \end{cases} \quad (2)$$

ε_v denotes the volumetric strain and k^b is the drained bulk modulus. Moreover, the Biot's tensor of a porous material can be expressed as a function of elastic properties of bulk skeleton and that of pore fluid. For an isotropic material, one gets:

$$b = 1 - \frac{k^b}{k^s}; \quad \frac{1}{M} = \frac{b-\phi}{k_s} + \frac{\phi}{k_f} \quad (3)$$

In this relation, k^s is the stiffness (volumetric modulus) of solid grains and k_f that of pore fluid. ϕ denotes the connected porosity. It is important to point out that when the porous material exhibit induced cracking (or damage), its elastic properties and porosity can evolve as functions of crack density. More precisely, the values of k^b, k^s and ϕ are not constant. On the other hand, when a cracked sample (thermally here) is subjected to hydrostatic compression, a part of micro-cracks are progressively closed. As a consequence, the effect of micro-cracks is attenuated (the so-called unilateral effect of crack closure) and the values of k^b and k^s can be partially restituted. This leads to the variation of elastic properties in terms of applied hydrostatic stress. Therefore, for a complete modeling of poroelastic behavior in damaging porous materials, a proper elastic damage model should be developed as shown in the previous studies [24]. Further, in order to identify the variation of elastic properties during hydrostatic compression, unloading–reloading cycles should be performed at different values of stress. However, this is beyond the topic of the present work. The emphasis here is the characterization of effects of thermally induced micro-cracks on the evolution of poroelastic properties of granite.

Therefore, the experimental program is simplified and only monotonic hydrostatic tests are performed. Accordingly, only two particular points of stress–strain curves are analyzed, namely the initial and asymptotic states. At the initial state, the slopes of stress–strain curve are used to define the initial bulk modulus and solid stiffness. At the asymptotic state, a quasi-linear stress–strain relation is obtained. The corresponding slopes are then used to define the asymptotic values of bulk modulus and solid stiffness. The corresponding values of Biot's coefficient are calculated and analyzed for these two states.

2.2 Material description and thermal treatment

The batch of granite samples were collected from Chuanshanpin Town, Hunan Province, China. According to the X-ray diffraction analysis in [34, 35], the mineral compositions of the granite are mainly composed of quartz (24.67%), albite (33.55%), microcline (37.16%), biotite (4.22%) and clinochlore (0.40%). The average porosity of granite in its natural state is 0.719% and its density is 2.621 g/cm^3. The gas permeability is about 1.941×10^{-18} m^2, the P-wave velocity is 4651.16 m/s and the thermal conductivity is 2.892w/(m K). The size of cylindrical samples is 50 mm × 100 mm. The sample preparation procedure fulfills the recommendation of the International Society of Rock Mechanics [10]. The selected samples did not contain apparent cracks.

The granite samples were first heated up to different values of temperature (200 °C, 400 °C, and 600 °C) and then cooled in water. More precisely, the samples were put in a muffle furnace for heating and the heating rate was set to 5 °C/min. The reached temperature was kept constant for 5 h. After the heating period, the samples were quickly placed into water for rapid cooling. (The temperature of water was about 20 °C and the volume about 25 L.) More details about the heating–cooling treatment can be found in [34, 35]. The cooled samples were further put in an oven at 105 °C for 24 h until completely dried. And the dried samples were conserved in sealed bags until they were used in mechanical tests.

2.3 Hydrostatic compression test

In this paper, compressive stresses and volumetric strains are denoted as positive values. Hydrostatic compression tests were performed on the treated granite samples under a room temperature between 20 °C and 25 °C. The used experimental device is shown in Fig. 1. As mentioned above, the main objective of the tests is to determine the values of k^b and k^s of the thermally treated granite samples at the initial and asymptotic states. To this end, two types

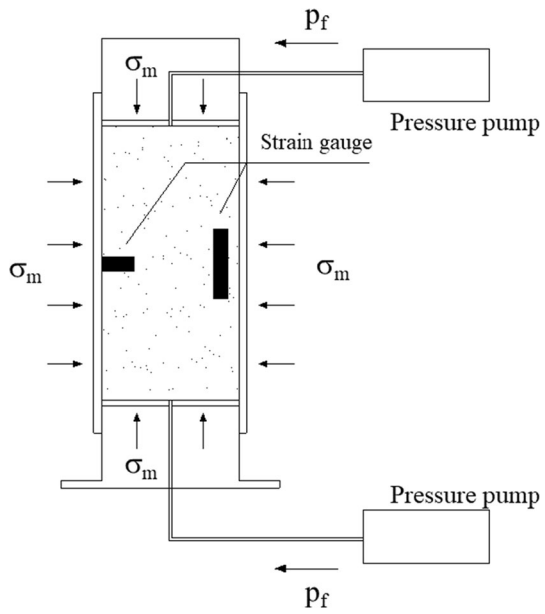

Fig. 1 Illustration of experimental device for hydrostatic poromechanical test

of loading path were used. During the first one, the compressive hydrostatic stress is applied under drained condition without pore pressure change ($\Delta p_f = 0$). The generated volumetric strain is measured. The obtained stress–strain curves are used for the calculation of initial and asymptotic values of bulk modulus. During the second loading path, the hydrostatic stress and pore pressure are increased simultaneously and equally ($\Delta p_f = \Delta \sigma_m$). The corresponding volumetric strain is also measured. As this volumetric strain is physically related to the compaction of solid grains, the stress–strain curves issued from this loading path are used for the calculation of initial and asymptotic values of solid stiffness.

3 Experimental results and discussions

3.1 Overall stress–strain behavior

By using the experimental procedure defined above, three tests were performed on three different samples for a given value of heating–cooling treatment temperature. Two sets of strain–strain curves are obtained for each test; the volumetric strain versus hydrostatic (or mean) stress curves and the volumetric strain of solid grains versus hydrostatic stress (or pore pressure) curves. Typical results obtained are presented in Fig. 2. One can see that relatively large scatters are observed between three tests performed for the same value of temperature. This is probably due to the initial differences between the tested samples. Moreover, the scatters are larger for the solid volumetric strain curves

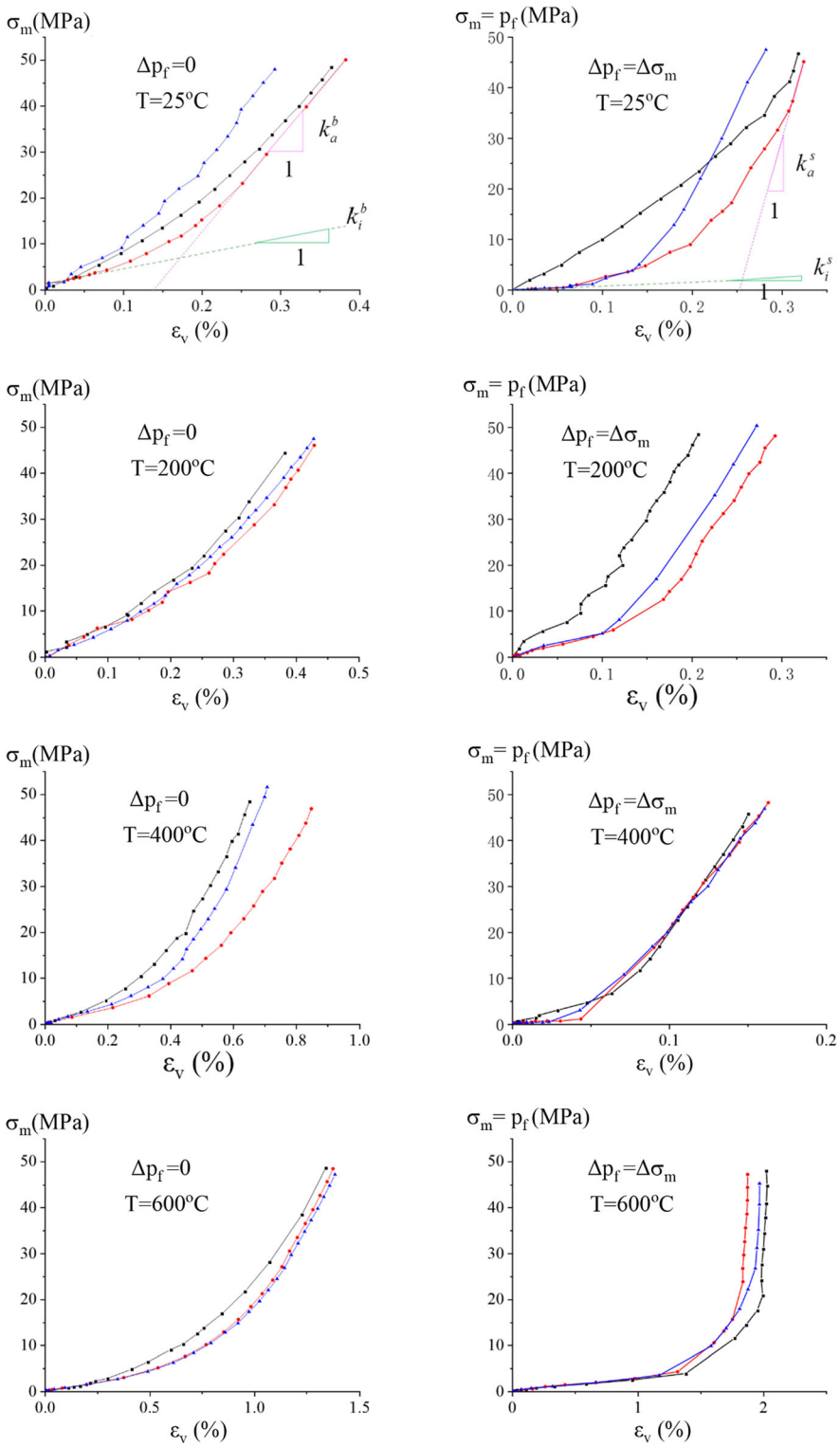

Fig. 2 Overall stress–strain curves during two steps of hydrostatic compression tests on samples with different heating–cooling treatment temperatures

($\Delta\sigma_m = \Delta p_f$) than for the bulk volumetric strain curves ($\Delta p_f = 0$). This seems to indicate that the material heterogeneity is mainly related to the solid grains. More interestedly, the scatters are more important for the samples treated under low temperature than for those treated under high temperature. For instance, the largest scatters

are observed for the samples which are not subjected to heating–cooling treatment (25 °C). It seems that due to the creation of micro-cracks inside the solid grains by the heating–cooling treatment, the material heterogeneity between the granite samples is attenuated.

On the other hand, for all the tested samples, strongly nonlinear concave stress–strain curves are obtained. The slope of volumetric strain curve defines the tangent elastic stiffness which is a function of applied stress. It is clear that the tangent elastic stiffness significantly increases with the applied stress due to the progressive closure of micro-cracks. When the applied stress is high enough, one obtains an asymptotic quasi-linear phase in almost each test. As mentioned above, the present study does not intend to establish a complete nonlinear elastic damage model. The objective is to quantify the effect of heating–cooling treatment on the poroelastic properties of granite. Therefore, only two quasi-elastic states are selected on the stress–strain curves: the initial state at the beginning of hydrostatic compression (the value of bulk modulus and solid stiffness are denoted as k_i^{b} and k_i^{s} respectively) and the asymptotic quasi-linear state at the end of loading (the values of bulk modulus and solid stiffness are denoted as k_a^{b} and k_a^{s} respectively). The obtained values are analyzed and discussed below.

3.2 Poroelastic properties at the initial state

The values of measured bulk modulus and solid stiffness at the initial state are given in Table 1. Their variations with the heating–cooling treatment temperature are presented in Fig. 3. It is worth noticing that at the beginning of loading, the applied stress is small enough to avoid closing micro-cracks. Therefore, the corresponding values of bulk modulus and solid stiffness are approximately considered as the elastic properties of the samples after the thermal treatment with different temperatures. In a general way but except the values of bulk modulus of three sound samples (at 25 °C and not subjected to thermal treatment), both the bulk modulus (k_i^{b}) and the stiffness of solid grains (k_i^{s}) significantly decreases with the temperature. This clearly indicates that a large number of micro-cracks are created in the granite samples during the heating–cooling treatment. The smallest value of bulk modulus and solid stiffness is both obtained for the samples treated at 600 °C. It is worth noticing that the bulk modulus is affected by both connected and occluded micro-cracks. However, the stiffness of solid grains is only affected by the occluded micro-cracks. The progressive diminution of initial solid stiffness shown in figure (b) clearly indicates that the thermal treatment not only generates connected but also occluded micro-cracks in the solid grains. And the quantity of occluded micro-cracks increases with the thermal treatment temperature. By using the values of k_i^{b} and k_i^{s}, the values of Biot's coefficient at the initial state are calculated by using the relation (3). The obtained values are also given in Table 1, and its evolution with temperature is shown in Fig. 4. Due to the large scatters of initial bulk modulus and solid stiffness for the natural samples (25 °C), the values of Biot's coefficient for these samples exhibit important scatters. However, considering the smallest value of Biot's coefficient obtained for the natural samples (this value appears to be mostly feasible according to the very low initial porosity of granite), a quasi-linear correlation (dotted line in Fig. 4) can still be found between the initial Biot's coefficient and thermal treatment temperature. The initial Biot's coefficient of granite is significantly amplified by the growth of both connected and occluded micro-cracks inside the solid grains, induced by the heating–cooling treatment.

Table 1 Experimental values of poroelastic properties at initial state

Temperature (°C)	Initial solid stiffness k_i^{s} (MPa)		Initial bulk modulus k_i^{b} (MPa)		Initial Biot's coefficient $b_i = 1 - k_i^{\mathrm{b}}/k_i^{\mathrm{s}}$	
	Value	Mean	Value	Mean	Value	Mean
25	3287.4	6535	664.3	3280	0.798	0.599
	6855.0		781.1		0.886	
	9463.5		8395.0		0.113	
200	8563.2	5997	5435.5	5186	0.365	0.202
	3982.1		4886.5			
	5445.6		5238.6		0.038	
400	6925.8	4005	2067.3	1870	0.702	0.579
	3648.9		1984.7		0.456	
	1442.9		1560.7			
600	921.4	1119	8.0	227	0.991	0.822
	1294.5		636.7		0.508	
	1143.0		37.9		0.967	

3.3 Poroelastic properties at the asymptotic linear state

The measured values of bulk modulus and solid stiffness at the asymptotic quasi-linear state are given in Table 2. Their variations with thermal treatment temperature are shown in Fig. 5. Compared with the results shown in Fig. 3 for the initial elastic state, it is seen that due to the closure of micro-cracks by applied compressive stress, the values of bulk modulus at the asymptotic state are significantly higher than those at the initial state. The experimental scatters are also significantly reduced. However, the bulk

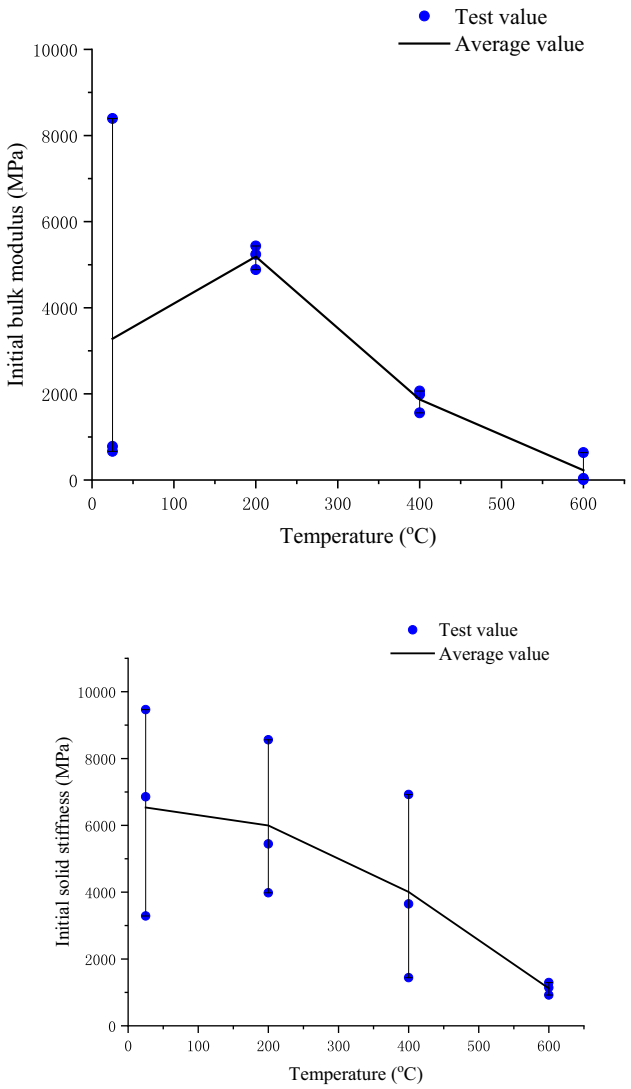

Fig. 3 Evolution of bulk modulus and stiffness of solid grains at the initial state with thermal treatment temperature

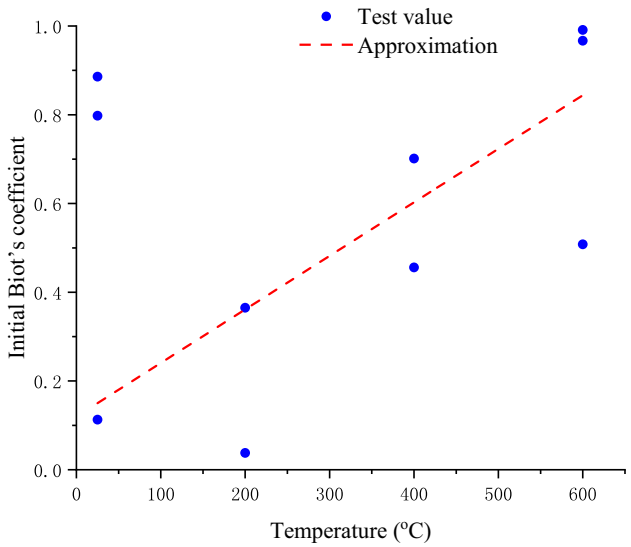

Fig. 4 Evolution of Biot's coefficient with thermal treatment temperature at the initial state

Table 2 Experimental values of poroelastic properties at asymptotic state

Temperature (°C)	Asymptotic solid stiffness k_a^s (MPa)		Asymptotic bulk modulus k_a^b (MPa)		Asymptotic Biot's coefficient $b_a = 1 - k_a^b/k_a^s$	
	Value	Mean	Value	Mean	Value	Mean
25	55,384.8	50,298	21,856.4	20,993	0.605	0.550
	62,966.1		20,667.5		0.672	
	32,545.5		20,457.4		0.371	
200	27,261.4	31,293	18,885.5	17,793	0.307	0.421
	36,462.7		17,312.9		0.525	
	30,157.6		17,180.6		0.430	
400	40,946.2	44,675	15,874.0	16,977	0.612	0.617
	50,473.3		16,717.7		0.669	
	42,606.1		18,340.2		0.570	
600	132,380.0	188,182	9232.7	9316	0.930	0.908
	382,486.0		9796.5		0.974	
	49,680.3		8918.7		0.820	

modulus at the asymptotic state still continuously decreases with the thermal treatment temperature. This indicates that only a part of micro-cracks are closed by the applied compressive stress and the remaining part is still interacting with connected porosity and affecting the bulk modulus. Moreover, according to some previous studies [7, 21, 22, 29], when the temperature is higher than 500 °C, the crystal structure of granite changes due to the phase transition of quartz. The crystal structure modification can also lead to the weakening of bulk modulus of granite. About the evolution of solid stiffness, it seems that its value remains almost constant until 400 °C and then increases. However, the values of the samples treated at 600 °C show important scatters. If we look at the two low values, it seems that the solid stiffness increases slightly between 400 °C and 600 °C. These results indicate that the majority of occluded micro-cracks inside the solid grains are closed by the applied compressive stress and pore pressure for the natural samples and the samples treated with 200 °C and 400 °C. For the samples treated at 600 °C, the increase in asymptotic solid stiffness is an interesting phenomenon. It seems that due to the high value of heating–cooling temperature, a high number of micro-cracks are created in the samples. The thermally induced cracks can create new fluid path ways between the initial occluded micro-cracks (and pores) and the connected ones. As a

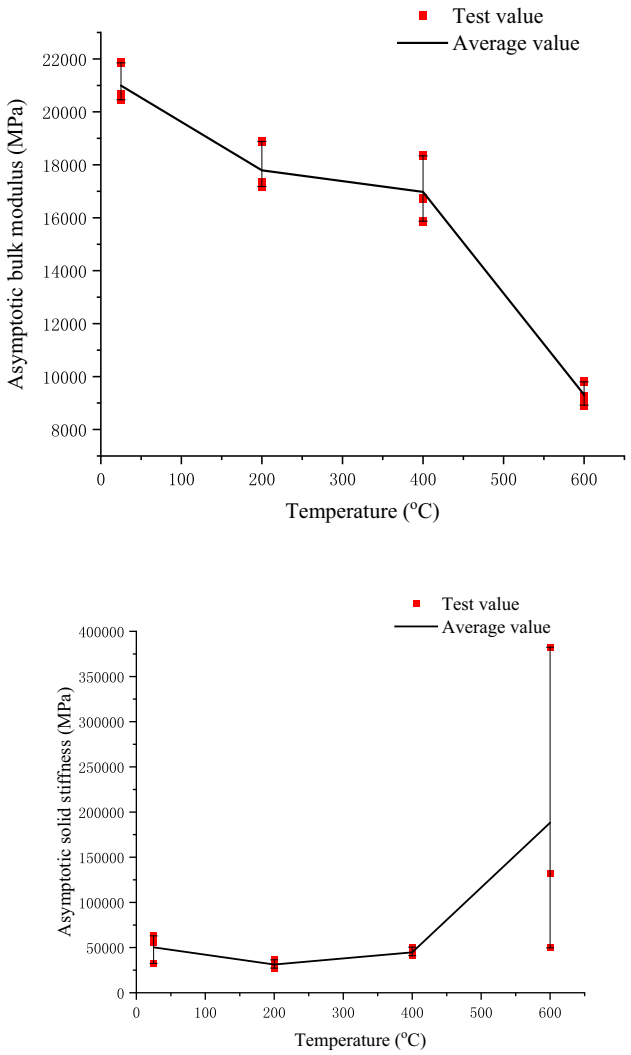

Fig. 5 Evolution of bulk modulus and stiffness of solid grains at the asymptotic state with thermal treatment temperature

consequence, during the second loading path, the injected fluid gets access to the newly connected cracks (and pores). The number of occluded micro-cracks inside the solid grains is reduced. This leads to the increase of stiffness of solid grains. Finally, the values of Biot's coefficient at the asymptotic linear state are calculated and given in Table 2. Its variations with thermal treatment temperature are presented in Fig. 6. Again, despite of the large experimental scatters obtained, a linear increasing evolution law can still be obtained as the first approximation. The Biot's coefficient at the asymptotic state also continuously increases with the heating–cooling temperature. This evolution is consistent with the progressive decrease in asymptotic bulk modulus and the increase of solid stiffness with the thermal treatment temperature. Furthermore, the comparison of Biot's coefficient evolution with temperature between the initial and asymptotic states is presented in Fig. 7. It is found that the difference of Biot's coefficient between the initial and asymptotic states is very small. But interestingly, the slope of variation with temperature is higher for the initial state than for the asymptotic state. It seems that the effect of heating–cooling on Biot's coefficient is stronger at the initial state but attenuated at the asymptotic state by the applied compressive hydrostatic stress and pore pressure. At low values of temperature, the value of asymptotic Biot's coefficient is higher than that at the initial state. This is due to the fact that a part of occluded micro-cracks at the initial state become connected ones at the asymptotic state due to the high increase in pore fluid pressure, leading to an increase in the solid stiffness. These results indicate that the Biot's coefficient of granite samples is more affected by the heating–cooling treatment than by the compressive stress loading.

4 Summary and conclusions

In this study, we have investigated the modification of poroelastic properties of granite samples subjected to heating–cooling treatment up to 600 °C. According to the results obtained, the following remarks can be drawn.

Natural granite samples contain a number of initial connected and occluded micro-cracks inside the solid grains. The heating–cooling treatment can generate a high number of additional micro-cracks in the solid grains, a part of them is occluded and another part is connected to initial cracks and pores. The presence of the occluded micro-cracks (or pores) significantly affects the variation of poroelastic properties of granite, in particular the stiffness of solid grains. Due to the micro-cracks induced by the

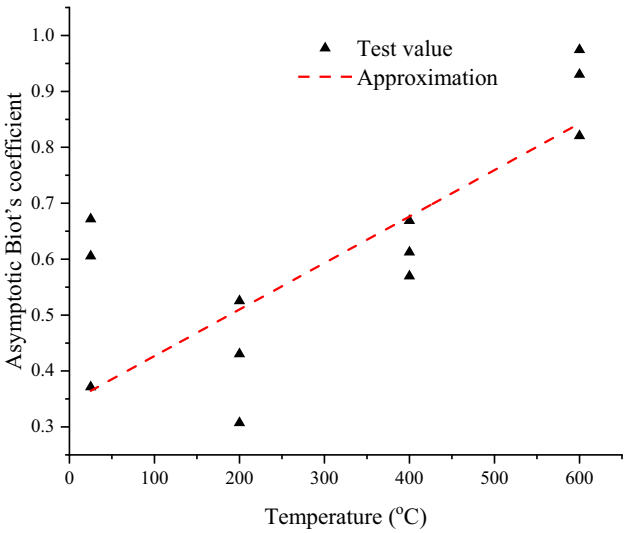

Fig. 6 Evolution of Biot's coefficient with thermal treatment temperature at the asymptotic state

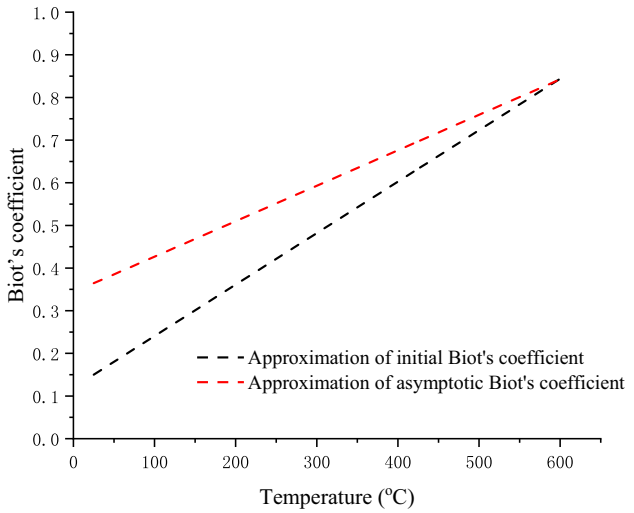

Fig. 7 Comparison of linear approximation of Biot's coefficient evolution with thermal treatment temperature between the initial and asymptotic states

thermal treatment, the bulk modulus of granite samples is significantly decreased. On the other hand, due to the thermally induced occluded micro-cracks, the stiffness of solid grains is also decreased. However, the decrease of solid stiffness can be compensated by the connection of initially occluded micro-cracks to the connected ones with the help of the thermally induced micro-cracks. This can lead to an increase of the stiffness of solid grains. As a consequence, for the studied granite, the decrease in the solid stiffness is smaller than that of the bulk modulus. Its Biot's coefficient exhibits a clear increase with the thermal treatment temperature.

During the subsequent hydrostatic compression loading until an asymptotic linear state is reached, a part of (both initial and thermally induced) connected and occluded micro-cracks are closed. This leads to a significant increase in both the bulk modulus and the stiffness of solid grains. However, due to the remaining part of open micro-cracks, the bulk modulus of granite remains affected by the thermal treatment and shows a continuous decrease with the temperature. The solid stiffness becomes almost constant for the samples treated by a temperature below 400 °C. This seems to indicate that the solid grains of the tested samples have a very similar micro-structure. However, the solid stiffness of the samples treated at 600 °C is higher than the other samples. This can be explained by the fact that a part of initially occluded micro-cracks become connected ones with the help of thermally induced micro-cracks in these samples. Finally, the Biot's coefficient at the asymptotic state remains affected by the heating–cooling treatment and continuously increases with the treatment temperature. The value of asymptotic Biot's coefficient (under compressive stress) is very close to that at the initial state (without compressive stress). Therefore, the Biot's coefficient of granite samples is essentially affected by the heating–cooling treatment rather than by the compressive stress.

Acknowledgements This work was jointly supported by the Natural Science Foundation of China (Grant numbers 51979100 and 51779252 and 51579093) and the National Key Research and Development Program of China (No. 2018YFC0809601).

References

1. Alam MM, Borre MK, Fabricius IL et al (2010) Biot's coefficient as an indicator of strength and porosity reduction: calcareous sediments from Kerguelen Plateau. J Petrol Sci Eng 70:282–297
2. Alm O, Jaktlund L (1985) The influence of microcrack density on the elastic and fracture mechanical properties of Stripa granite. Phys Earth Planet Interiors 40(3):161–179
3. Baisch S, Weidler R, Voros R et al (2007) Induced seismicity during the stimulation of a geothermal HFR reservoir in the Cooper Basin, Australia. Bull Seismol Soc Am 96:2242–2256
4. Biot MA (1941) General theory of three-dimensional consolidation. J Appl Phys 12:155–164
5. Biot MA, Willis DG (1957) The elastic coefficients of the theory of consolidation. J Appl Mech 24:594–601
6. Bishop AW (1973) The influence of an undrained change in stress on the pore pressure in porous media of low compressibility. Geotechnique 23:435–442
7. Chaki S, Takarli M, Agbodjan WP (2008) Influence of thermal damage on physical properties of a granite rock: porosity, permeability and ultrasonic wave evolutions. Constr Build Mater 22:1456–1461
8. Cheng AHD (1997) Material coefficients of anisotropic poroelasticity. Int J Rock Mech Min Sci 34:199–205
9. Ersoy A, Waller MD (1995) Textural characterisation of rocks. Eng Geol 39:123–136
10. Franklin JA, Vogler UW, Szlavin J (1979) Suggested methods for determining water content, porosity, density, absorption and related properties and swelling and slake-durability index properties. Part 1: Suggested method for determining water content, porosity, density, absorption and related properties. Int J Rock Mech Min Sci Geomech Abstr 16:143–151
11. Géraud Y, Mazerolle F, Raynaud S (1992) Comparison between connected and overall porosity of thermally stressed granites. J Struct Geol 14:981–990
12. Han G, Jing H, Su H et al (2019) Effects of thermal shock due to rapid cooling on the mechanical properties of sandstone. Environ Earth Sci 78:146
13. Heap MJ, Violay M, Wadsworth FB et al (2017) From rock to magma and back again: the evolution of temperature and deformation mechanism in conduit margin zones. Earth Planet Sci Lett 463:92–100
14. Kohl T, Evans KF, Hopkirk RJ et al (1995) Coupled hydraulic, thermal and mechanical considerations for the simulation of hot dry rock reservoirs. Geothermics 24:345–359
15. Lade PV, De Boer R (1997) The concept of effective stress for soil, concrete and rock. Geotechnique 47:61–78
16. Lu C, Wang G (2015) Current status and prospect of hot dry rock research. Sci Technol Rev 33:13–21
17. Ma Z (2008) Experimental investigation into Biot's coefficient and rock elastic moduli. Oil Gas Geol 01:135–140
18. Meredith PG, Atkinson BK (1985) Fracture toughness and subcritical crack growth during high-temperature tensile deformation

of Westerly granite and Black gabbro. Phys Earth Planet Infer 39:33–51
19. Merriam R, Rieke HH (1970) Young Tensile strength related to mineralogy and texture of some granitic rocks. Eng Geol 4:155–160
20. Mian C, Zhida C (1999) Effective stress laws for multi-porosity media. Appl Math Mech 20:1207–1213
21. Nasseri MHB, Tatone BSA, Grasselli G et al (2009) Fracture toughness and fracture roughness interrelationship in thermally treated westerly granite. Pure Appl Geophys 166:801–822
22. Nasseri MHB, Schubnel A, Benson PM et al (2009) Common evolution of mechanical and transport properties in thermally cracked westerly granite at elevated hydrostatic pressure. Pure Appl Geophys 166:927–948
23. Nur A, Byerlee J (1971) An exact effective stress law for elastic deformation of rocks with fluids. J Geophys Res 76:6414–6419
24. Shao JF (1998) Poroelastic behaviour of brittle rock materials with anisotropic damage. Mech Mater 30:41–53
25. Terzaghi K (1923) Die Berechnung der Durchlassigkeitziffer des Tones aus dem Verlauf der hydrodynamischen Spannungserscheinungen. Sitzungsber Akad Wiss Wien 132:125–138
26. Tester JW, Anderson BJ, Batchelor AS et al (2006) The future of geothermal energy. Massachusetts Institute of Technology, Cambridge
27. Tugrul A, Zarif IH (1999) Correlation of mineralogical and textural characteristics with engineering properties of selected granitic rocks from Turkey. Eng Geol 51:303–317
28. Xi B, Zhao Y (2010) Experimental research on mechanical properties of water-cooled granite under high temperatures within 600°C. Chin J Rock Mech Eng 29(5):892–898
29. Xi D (1994) Physical properties of mineral phase transition in granite. Acta Mineralogica Sinica 14:223–227
30. Wu X, Huang Z, Zhang S et al (2019) Damage analysis of high-temperature rocks subjected to LN2 thermal shock. Rock Mech Rock Eng 52(8):1–19
31. Yuan H, Agostini F, Duan Z et al (2017) Measurement of Biot's coefficient for COx argillite using gas pressure technique. Int J Rock Mech Min Sci 92:72–80
32. Yang R, Huang Z, Shi Y et al (2019) Laboratory investigation on cryogenic fracturing of hot dry rock under triaxial-confining stresses. Geothermics 79:46–60
33. Zhao Y, Borja RI (2020) A continuum framework for coupled solid deformation-fluid flow through anisotropic elastoplastic porous media. Comput Methods Appl Mech Eng 369:113225
34. Zhang F, Zhao J, Hu D, Skoczylas F, Shao JF (2018) Laboratory investigation on physical and mechanical properties of granite after heating and water-cooling treatment. Rock Mech Rock Eng 51:677–694
35. Zhang F, Zhao J, Hu D, Shao JF, Sheng Q (2019) Evolution of bulk compressibility and permeability of granite due to thermal cracking. Geotechnique 69:906–916
36. Zhang W, Sun Q, Hao S et al (2016) Experimental study on the variation of physical and mechanical properties of rock after high temperature treatment. Appl Therm Eng 98:1297–1304